

Stearate intercalated layered double hydroxides: effect on the physical properties of dextrin-alginate films

E. P. LANDMAN, W. W. FOCKE*

Institute of Applied Materials, University of Pretoria, Pretoria 0002, Republic of South Africa
E-mail: walter.focke@up.ac.za

Published online: 22 April 2006

Glycerol-plasticized dextrin-alginate films were prepared by solution casting. They contained a fixed amount (16.6% mass/dry film mass) of functional filler based on the reaction products of the LDH, $\text{Mg}_4\text{Al}_2(\text{OH})_{12}\text{CO}_3 \cdot 3\text{H}_2\text{O}$, and stearic acid (SA). The films were characterized using infrared (IR) spectroscopy, scanning electron microscopy (SEM) and X-ray diffraction (XRD). The effect of filler composition on water vapour permeability and film stiffness was determined. The ratio of stearic acid (SA) to the LDH ($\text{Mg}_4\text{Al}_2(\text{OH})_{12}\text{CO}_3 \cdot 3\text{H}_2\text{O}$) was varied over the full composition range. Infrared spectroscopy and X-ray diffraction studies confirmed that the SA intercalated into the LDH. The Young's modulus of films attained a maximum value (more than double the value for the neat film) at a filler composition of 60% SA. The water vapour permeability showed a broad minimum at filler compositions of 50–80% SA. Scanning electron microscopy revealed that in this composition range the filler assumes a high-aspect-ratio platelet morphology. This contrasts with the sand rose morphology of the LDH starting material and the globular dispersion of 100% SA in the film.

© 2006 Springer Science + Business Media, Inc.

1. Introduction

Edible films and coatings are used to protect foodstuff from water vapour and oxygen in their environment. Such films also prevent water moving from one part to another in multi-component foodstuffs, for example to separate the filling or sauce from the dough of pizzas or pies. Most edible film-forming polymers or hydrocolloids (such as starch, sodium alginate, and sodium caseinate) are hydrophilic. They pose virtually no barrier against water vapour and become soggy in contact with liquid water. Lipid films are good barriers against water, but have little structural integrity. This problem has been overcome using laminates of hydrocolloid and wax films and also by making emulsions of the wax or lipid within the hydrocolloid solution. Waxes such as beeswax and stearic acid are emulsified within the surface-active sodium alginate or sodium caseinate and their blends with starch [1–3].

Polymer-layered clay nanocomposites are filled polymers in which at least one of the dimensions of the filler is in the nanometre range. Nanocomposites in general have increased modulus, strength and heat resistance, as well as decreased gas permeability and flammability in com-

parison to the pristine polymer [4]. Studies were done on preparing composites of starch with kaolin [5], Ca^{2+} hectorite [6] and kaolinite, hectorite, layered double hydroxide (LDH) and brucite [7]. These studies focused mainly on the mechanical properties and microstructure of the composites as well as determining whether exfoliation took place by means of X-ray diffraction. Such platelet fillers can also be used to reduce the WVP of hydrophilic polymers such as starch or alginate.

The water vapour permeability (WVP) and also the permeability of large organic molecules (or pharmaceuticals) in sodium alginate and sodium caseinate films can be reduced by cross-linking with polyvalent cations, e.g. Ca^{2+} . This can be done by immersing films in solutions of Ca^{2+} salts [3] or by *in situ* leaching of Ca^{2+} ions from insoluble CaCO_3 by acids [8]. This mechanism might play a role in the current system that is composed of an insoluble layered double hydroxide and stearic acid.

Hydrotalcite is an anionic clay mineral with the composition $\text{Mg}_6\text{Al}_2(\text{OH})_{16}\text{CO}_3 \cdot 4\text{H}_2\text{O}$. It has the same layered structure as brucite [$\text{Mg}(\text{OH})_2$] but with some of the Mg^{2+} ions substituted by Al^{3+} ions. The presence of the Al^{3+}

*Author to whom all correspondence should be addressed.

TABLE I Components of the films and their roles

Component name	Supplier	Role
Dextrin, Stydex 074030	African Products (Pty.) Ltd. South Africa	Biodegradable polymer
Sodium Alginate (E401), Manugel GMB, viscosity of 1% aqueous solution is 185 cP.	Kelco International Limited	Biodegradable polymer, film former, emulsion stabilizer (due to high viscosity), prevents agglomeration of LDH-SA
99% Glycerol	Merck, UNILAB®	Plasticizer
85% Stearic acid	Merck	Hydrophobic, intercalate into LDH
LDH, Mg ₄ Al ₂ (OH) ₁₂ CO ₃ ·3H ₂ O Particle size distribution by Mastersizer 2000 (Malvern Instruments): d(0.1): 0.694 μm; d(0.5): 5.062 μm and d(0.9): 23.925 μm.	Chamotte Holdings (Pty.) Ltd., South Africa	Filler, intercalated by SA
Talc	Sigma-Aldrich, <10 micron, 3MgO·4SiO ₂ ·H ₂ O	Filler, cannot be intercalated by SA. Coated and dispersed
Bentonite Ocean Clear	Boland Base Minerals, South Africa	Filler, cannot be intercalated by SA, coated and dispersed by SA
Foamaster 8034	Cognis	Prevents foam formation due to CO ₂ release.
Deionised water or tap water		Solvent
Ethanol, rectified 96%	Dana Chemicals	Solvent

ions gives rise to a residual positive charge in the layers. This positive charge is balanced by anions such as CO₃²⁻, Cl⁻ and NO₃⁻ or organic anions in the interlayer [9]. A range of compositions is possible in terms of bivalent and trivalent cations and their relative amounts. These types of compounds are more generally referred to as layered double hydroxides (LDHs).

In the present study a combination of an LDH [Mg₄Al₂(OH)₁₂CO₃·3H₂O] and stearic acid (SA) was used to reduce the WVP of glycerol-plasticized dextrin-alginate films. Ideally the SA would intercalate into the LDH structure to form LDH-SA during the film solution preparation. Stearate and other surfactant intercalated LDHs have large, plate-like microscopic structures [10, 11]. Such extended plate-like structures could lower the WVP of the dextrin-alginate films depending on their relative orientation within the films.

2. Experimental

2.1. Materials

The materials used, their source of origin, and their respective roles are given in Table I.

2.2. Film preparation procedure

Wu *et al.* [1] attempted to lower the WVP of starch-alginate films by using, amongst others, SA. Their recipe was followed (Table II) except that the lecithin emulsifier was omitted and LDH, Mg₄Al₂(OH)₁₂CO₃·3H₂O, was included instead. The ratio of SA and LDH was varied to determine its effect on WVP and Young's modulus. The SA and LDH together are referred to as the filler. It can consist of 100% SA, 100% LDH or any ratio in between. The filler content was kept constant at 16.6% mass/mass of the dried film, approximately the same as the amount of SA used by Wu *et al.* [1]. Films are referred to in terms of the SA content of the filler in the Figures and by annotations such as 60SA/40LDH for a film where the filler consists of 60% SA and 40% LDH by mass.

Dextrin, sodium alginate and the LDH were crushed and mixed using a mortar and pestle. This shearing action in this procedure helped to break down LDH agglomerates. The presence of the LDH aided subsequent dissolution of the alginate by preventing lump formation. The powdered mixture was slowly added to the water, ethanol, glycerol and SA solution at 78°C. The mixture was stirred continuously and a reaction time of one hour was used throughout. CO₂ is released during the intercalation of stearate into LDH and this necessitated the use of a defoamer. Although this was an effective strategy, the mixtures were nevertheless ultrasonicated in warm water to ensure complete release of trapped bubbles. 8 g portions of the solutions were cast into metal rings of approximately 67 mm diameter to prepare samples for WVP analyses. 45 g portions were cast into 150 mm square metal holders that were placed on a non-stick silicone sheet (Silicone zone®). The samples were left to dry at room temperature and then removed by peeling. The films were cut into 45 mm diameter circles for WVP tests or punched into dumbbell shapes (6 mm wide, 35 mm gauge length, 115 mm total length) for tensile testing. Samples were conditioned at 23 ± 2°C, 75% RH (saturated NaCl solution [12]) prior to analysis.

TABLE II Relative amounts of the different components in the films solutions and dry films

Constituent	Typical amounts/(g)	% in film solution	% in dried film
Dextrin	2.5	2.78	41.39
Sodium alginate	1	1.11	16.56
Glycerol	1.4	1.55	23.18
SA	0–1	0–1.11	0–16.56
LDH	1–0	1.11–0	16.56–0
Defoamer	0.14	0.16	2.32
Water	60	66.64	–
Ethanol	24	26.65	–

One film was prepared using tap water to determine whether the Ca^{2+} ions it contains would have a negative effect (by reducing the alginate solubility) or a positive effect (by cross-linking the alginate) on the WVP.

2.3. Characterization

2.3.1. Fourier Transform Infrared Spectroscopy (FTIR)

A Perkin Elmer Spectrum RX I FT-IR System was used to scan the infrared transmittance through a KBr (Uvasol, potassium bromide, Merck) pellet 32 times at a resolution of 2 cm^{-1} . The averaged spectrum was background-corrected using a pure KBr pellet run under similar conditions. The pellets were prepared with approximately 2 mg of sample and 100 mg of KBr. The 2 mg powder samples were obtained by diluting the film solution with excess deionised water in order to release the insoluble LDH-SA. It was subsequently recovered by centrifugation, dried and ground. This was done in order to enable the observation of carboxylate vibrations of the intercalated stearate, which is otherwise overshadowed by the carboxylate peaks of the sodium alginate.

2.3.2. Powder X-ray Diffraction (XRD)

The XRD analyses were done on a Siemens D500 X-ray system equipped with a 2.2 kW Cu long fine focus tube, variable slit and secondary graphite monochromator. The system is computer controlled using SIEMENS DIFFRAC^{Plus} software. The goniometer was set to reflection mode. The films were placed on a no-background silicon (Si) wafer before placing it onto the aluminium sample holder to prevent aluminium peaks from being seen. Samples were scanned from 1 to $40^\circ 2\theta$ with Cu K radiation (1.5418 \AA) at a speed of $0.02^\circ 2\theta$, with a recording time of 2 s per step and generator settings of 40 kV and 30 mA.

2.3.3. Scanning Electron Microscopy (SEM)

The film samples were freeze fractured by dipping into liquid nitrogen and then breaking the brittle film. The broken cross-sections of the films were studied. These were coated with chromium in a high resolution ion beam coater (Gatan Model 681, Warrendale, USA) to prevent charge build-up due to its low conductivity. Samples were then studied with a JSM-6000F field emission scanning electron microscope (JEOL, Tokyo, Japan).

2.3.4. Water vapour permeability (WVP)

The cast and dried films were cut into discs of appropriate size for the WVP cups. A Mitutoyo Digimatic Indicator was used to determine the thickness of each disc at 9 positions. The measured thicknesses varied between 130 and $140\text{ }\mu\text{m}$. Additional samples were prepared in order to determine the effect of film thickness and composition

on the WVP. In all cases at least four discs per formulation were tested. Film discs were mounted on cups filled with dried silica gel and placed in a desiccator filled with saturated NaCl solution in contact with excess NaCl to obtain 75% relative humidity (RH) at $23 \pm 2^\circ\text{C}$ [12]. Films derived from emulsions always have a shiny side (bottom) and a dull side due to accumulation of lower density wax (or fatty acid) at the top. Therefore, the measured WVP depended on which side faced which relative humidity [3]. Care was taken to always place the shiny (more hydrophilic) side facing the 0% RH side.

The WVP of the best performing film was also measured at $38^\circ\text{C}/90\% \text{RH}$ to allow performance classification (good, moderate or poor) according to the scheme of Krochta *et al.* [13].

2.3.5. Tensile properties

Films were conditioned for at least two weeks before testing to ensure that results would be comparable in terms of the sample ages. Reported sample thicknesses are averages of measurements made at three positions within the middle portion of the dumbbells. Measured thicknesses ranged from 110 to $130\text{ }\mu\text{m}$. Samples were tested at a strain rate of 1 mm/min on a LRX Plus instrument from Lloyd Instruments. Tests were performed at 25°C at ambient humidity (30–50% RH). Three samples of each formulation were tested and averaged. The results were analysed using Nexygen software.

3. Results and Discussion

3.1. Fourier Transform Infrared spectroscopy (FTIR)

The FTIR spectrum of the LDH-SA intercalates obtained from the 60SA/40LDH film is shown in Fig. 1. The absence of the $\nu(\text{C}=\text{O})$ stretching vibration at 1702 cm^{-1} reveals that there is no free stearic acid in the sample. The carboxylate (COO^-) asymmetric stretching vibrations at 1539 cm^{-1} , 1554 cm^{-1} and 1576 cm^{-1} correspond closely with those reported by Borja *et al.* [14] for meristate inter-

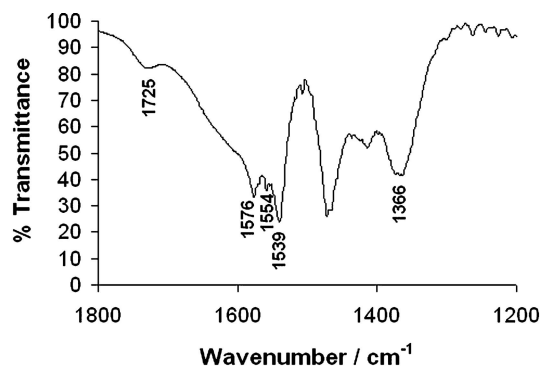


Figure 1 FTIR spectrum of the LDH-SA intercalates isolated from the 60SA/40LDH film solution, indicating complete ionisation and intercalation of SA together with some carbonate anions (1366 cm^{-1}).

calated $\text{Mg}_3\text{Al-LDH}$ (1542 cm^{-1} , 1557 cm^{-1} and 1589 cm^{-1}). The weak peak at 1725 cm^{-1} was also seen by Borja *et al.* [14] at 1720 cm^{-1} and can be attributed to the intercalation of the free acid (COOH). It is concluded that a similar intercalation product was obtained in the current aqueous film solutions as was obtained by Borja *et al.* [14] via the ion exchange of the Cl^- ion in LDH-Cl with fatty acids dissolved in ethanol. Some unreacted carbonate counter-ions always remained in the LDH (vibration at 1366 cm^{-1}) no matter how much SA was used.

3.2. Water vapour permeability (WVP)

The water permeability of hydrophilic films depends on the film moisture content. In the WVP experiment the film separates a region of high humidity from one of very low humidity. Therefore there is also a gradient in the moisture content across the film. Owing to concentration polarization, this gradient depends on the film thickness. The consequence is that, unlike hydrophobic polymer films, the WVP of hydrophilic films depends on film thickness. This was previously noted by McHugh *et al.* [15].

Fig. 2 shows the WVP of several films. The WVP of blank films (only dextrin, alginate and glycerol, no LDH or SA) and films containing only SA or only LDH as filler varied linearly with film thickness. The WVP of films containing combinations of LDH and SA were lower and it appeared to be independent of film thickness.

Fig. 3 shows the effect of filler composition on the WVP of films of a fixed thickness. A broad minimum in the WVP is observed at filler compositions ranging from 80SA/20LDH to 50SA/50LDH (Fig. 3). The film with 100% SA as the filler, showed only a 17% decrease in the WVP relative to the blank film. This value accords well with the results obtained by Wu *et al.* [1]. However, the replacement of even 20% of the SA with LDH decreased the WVP by 80% relative to that of the blank film (Fig. 3).

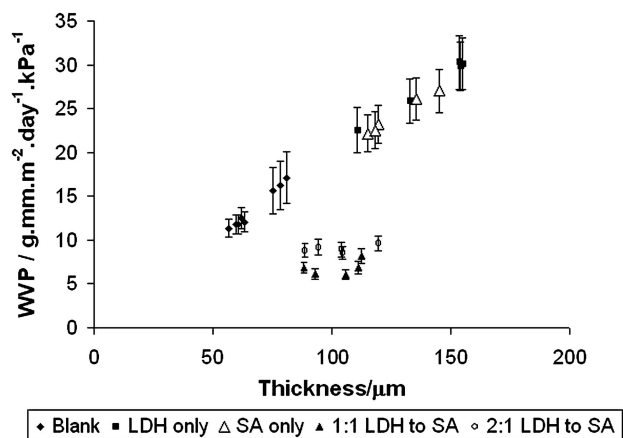


Figure 2 Thickness dependence of WVP of films with no filler, SA only or LDH only showing hydrophilic tendencies and those with combinations of SA and LDH showing hydrophobic tendencies.

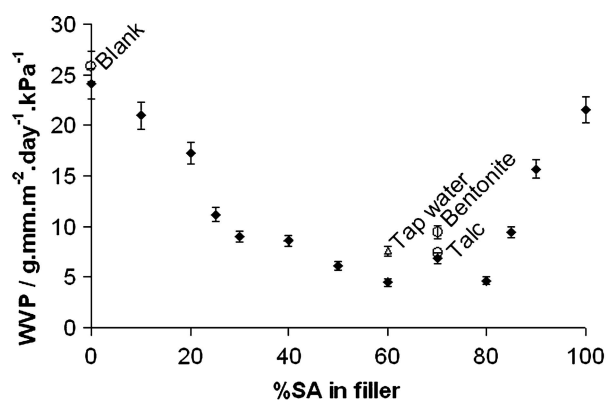


Figure 3 WVP measurements of constant-thickness films with fillers varying from 100SA/0LDH to 0SA/100LDH, showing a wide range of filler compositions yielding a minimum in the WVP.

The Ca^{2+} and perhaps also the Mg^{2+} ions present in tap water could cause cross-linking of the alginate and thereby improve WVP. However, premature cross-linking impairs the alginate solubility and this would be detrimental to film formation. Fig. 3 shows that using of tap water had no detrimental effects on the results. This implies that it might not be necessary to demineralise or deionise the water for large-scale applications.

The 60SA/40LDH film had a WVP of $13.5 \pm 0.5\text{ g}\cdot\text{mm}\cdot\text{m}^{-2}\cdot\text{day}^{-1}\cdot\text{kPa}^{-1}$ when tested at 38°C and 90% RH. This is border line between the poor ($10\text{--}100\text{ g}\cdot\text{mm}\cdot\text{m}^{-2}\cdot\text{day}^{-1}\cdot\text{kPa}^{-1}$) and moderate ($0.1\text{--}10\text{ g}\cdot\text{mm}\cdot\text{m}^{-2}\cdot\text{day}^{-1}\cdot\text{kPa}^{-1}$) WVP categories defined by Krochta *et al.* [13].

3.3. Scanning Electron Microscopy (SEM)

The microstructures of some of the films are shown in Fig. 4. SA, as the sole filler, dispersed as globules within the film (Fig. 4A). This explains why it did not alter the WVP significantly. The decrease in WVP (Fig. 3) coincides with the appearance in the film of aligned platelets, approximately $100\text{--}200\text{ nm}$ thick and $>20\text{ }\mu\text{m}$ long (Fig. 4B and C). Such flat structures have previously been encountered with surfactant intercalated LDHs [10, 11]. This morphology is in stark contrast with the original sand rose morphology of the LDH starting material shown in Fig. 4D.

Beyond the filler composition of 50SA/50LDH, the platelet structures gradually disappeared and the WVP increased to higher values. Films incorporating sheet-like fillers such as talc at the same mass % dosage level showed similar WVP (Fig. 3). The improved barrier properties of the films containing both SA and LDH are therefore attributed to the formation of aligned high-aspect ratio sheets of SA intercalated LDH. Note that, when no sodium alginate was present, the LDH-SA intercalates tended to agglomerate in starch or dextrin solutions. This suggests that sodium alginate acts as an efficient dispersant for LDH sheets in the matrices considered.

3.4. X-ray Diffraction (XRD)

The broad hump centred around $20^\circ 2\theta$ in the XRD spectrum of the blank film (no LDH or SA) indicates an amorphous structure. The 100SA/0LDH film had a reflection at around 40 \AA (due to the stearic acid bilayer, polymorph C [17]) and a small peak at about 8.1 \AA due to the forma-

tion of alginic acid crystals (2-fold screw axis with fiber period of 8.7 \AA , [18]).

Depending on the temperature and the relative amount of stearate present, either a monolayer or bilayer intercalated LDH may form (Fig. 5). The interlayer distance is 32 \AA for the monolayer and $52\text{--}53 \text{ \AA}$ for the bilayer [10,

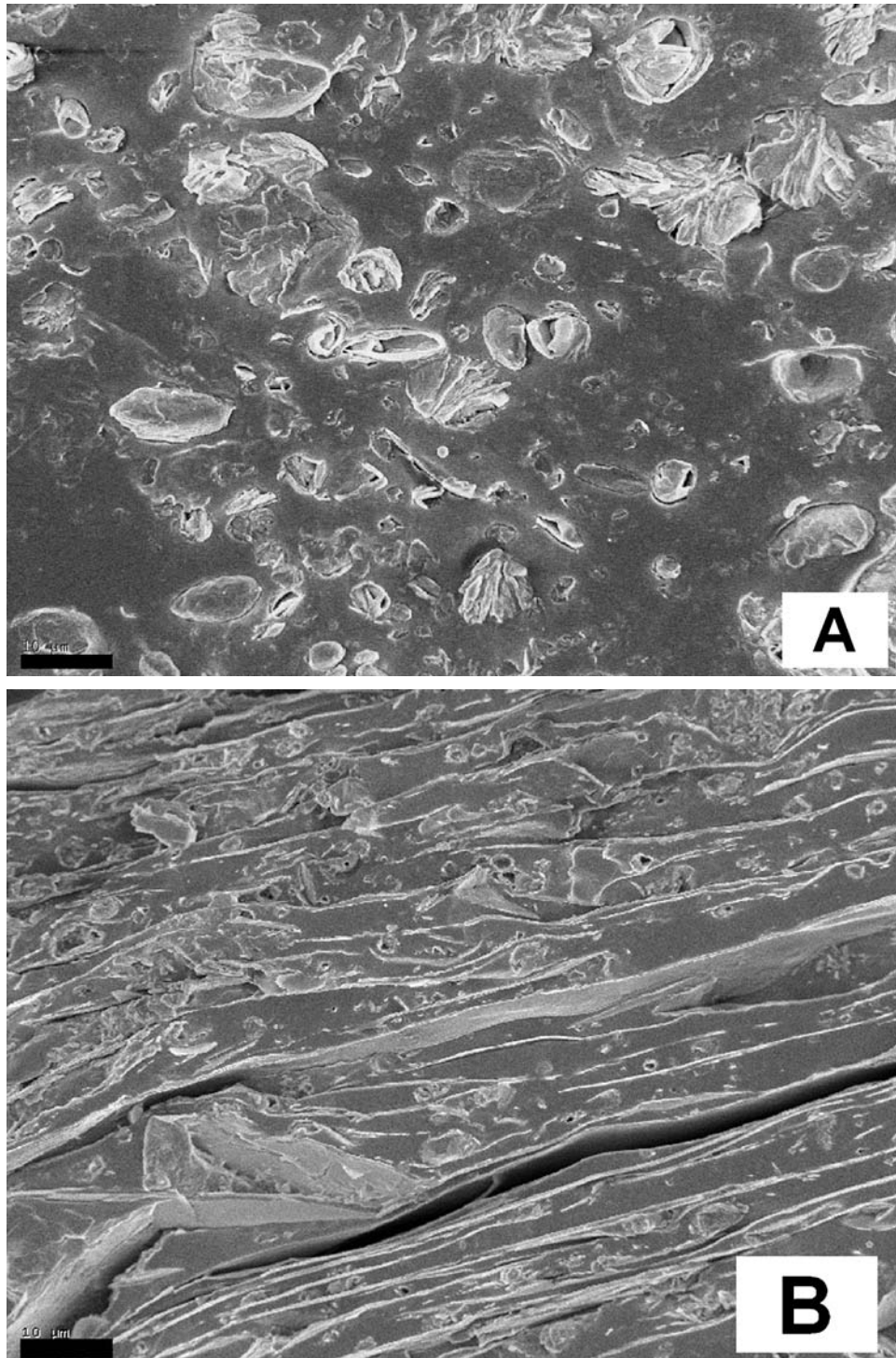


Figure 4 Scanning electron micrographs of the films. (A) 100SA/0LDH. Bar is $10 \mu\text{m}$. (B) 60SA/40LDH. The LDH-SA intercalate formed long, flat structures. Bar is $10 \mu\text{m}$. (C) Large magnification of 60SA/40LDH showing thickness of plates. Bar is $0.1 \mu\text{m}$. (D) Sand-rose structure of the LDH powder. Bar is $2 \mu\text{m}$. (Continue on next page)

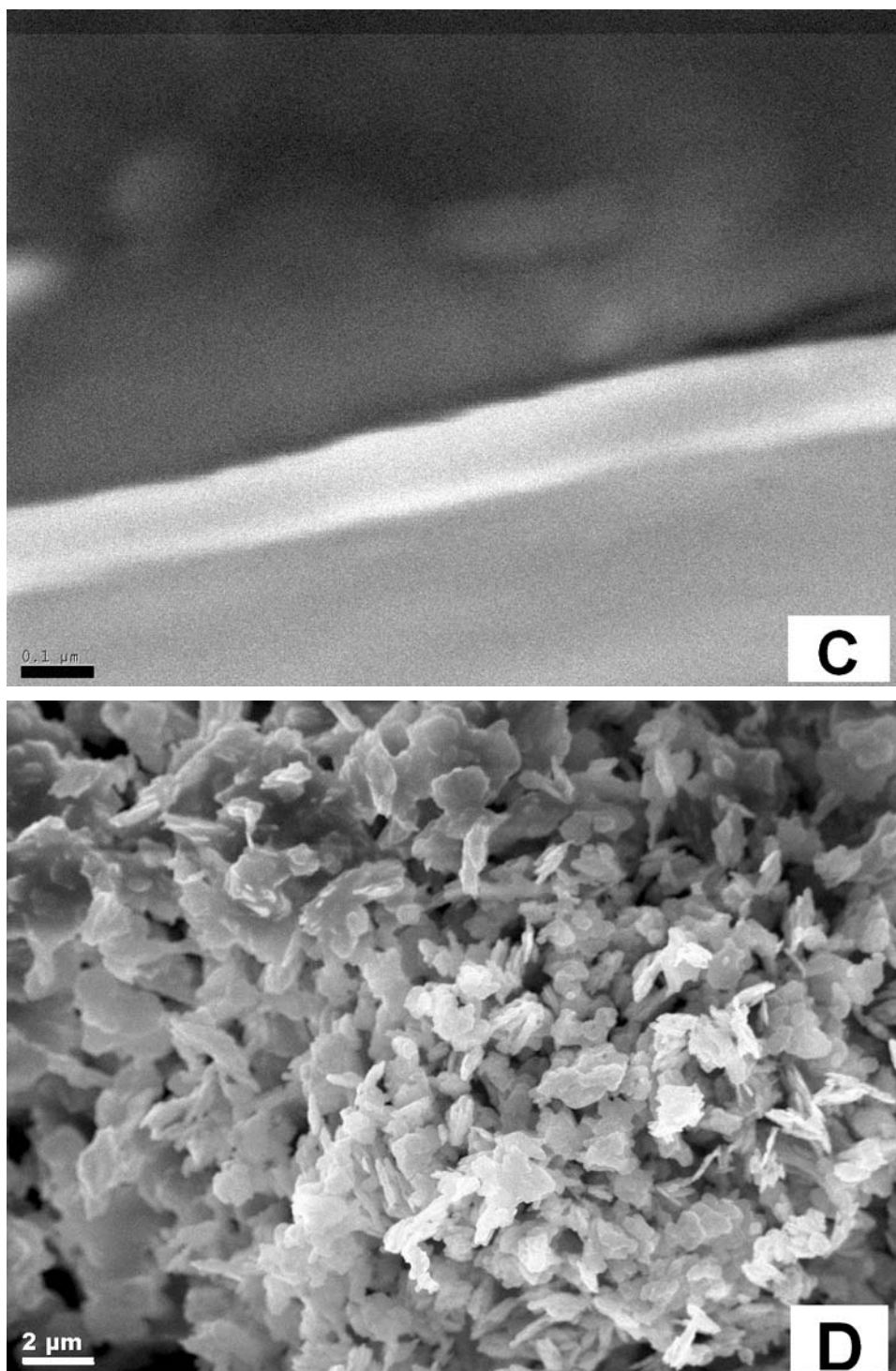


Figure 4 Continued.

16]. Upon the addition of LDH to the SA in the film, an interlayer distance of 53 \AA was reached at the filler composition of 80SA/20LDH (80% SA, Fig. 7). With increasing LDH the intensity of the basal reflection and the interlayer distance decreased (Figs. 6 and 7). It was expected that the interlayer distance would have remained at ca. 53 \AA in the 60SA/40LDH and 70SA/30LDH films as bilayer forms were expected to form. However, the XRD traces showed a lower intensity peak corresponding to a lesser interlayer-

distance phase. The reasons for this observation are not understood at present. It might be that the higher interlayer distance reflections weakened owing to exfoliation or delamination. Differences in the relative orientation of platelets inside the film could also provide an explanation.

At the filler composition of 50SA/50LDH, the basal reflection at 54 \AA reappeared. Further lowering of the SA to LDH ratio caused a continuous decrease in the observed interlayer distance ($45\text{--}52 \text{ \AA}$). This indicates that

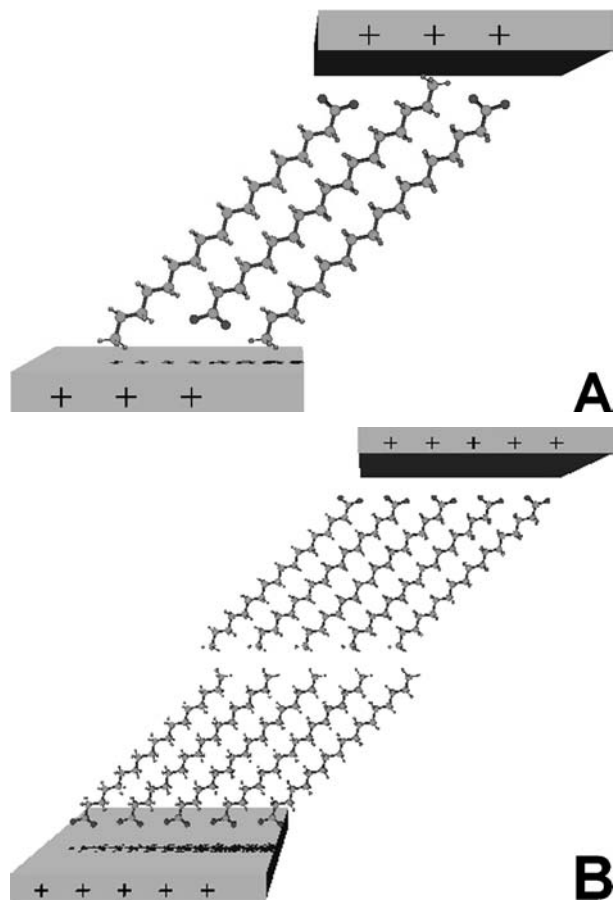


Figure 5 Monolayer (A) and bilayer (B) arrangement of stearate intercalated within LDH.

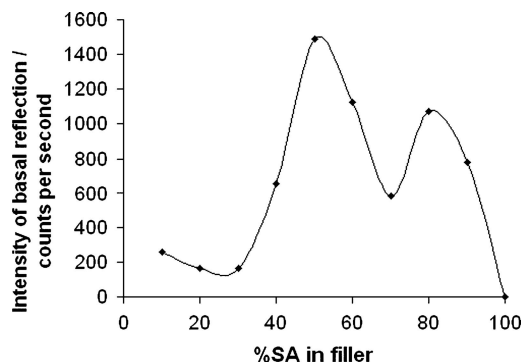


Figure 6 Variation in intensity of the basal reflection of the intercalated phase (LDH-SA) as function of filler composition. The dip in intensity indicated that exfoliation (delamination) took place.

the SA intercalated in forms intermediate to the mono- and bilayer arrangements.

Fig. 8 shows the time dependent evolution of the crystalline phases present in the 70SA/30LDH film. At 10 min amorphous phases predominate. The LDH basal reflection at 7.7 \AA had a low intensity, because the LDH particles were still mostly agglomerated, settling to the bottom and not forming part of the cast film. At 30 min the sand-rose structures had broken down and the LDH particulates were suspended in the film solution. The 7.7 \AA reflection

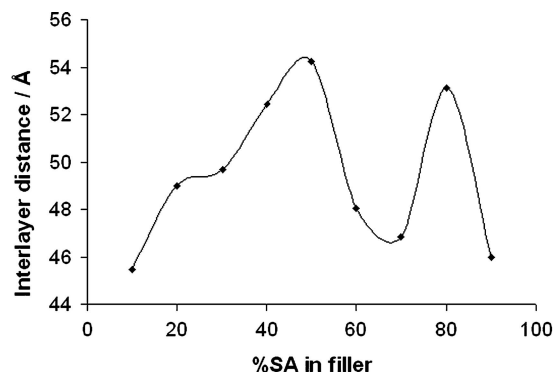


Figure 7 Variation of the interlayer distance of the intercalated phase (LDH-SA) as function of the filler composition. The dip in interlayer distance indicated that exfoliation took place, leaving only a phase with smaller interlayer distance.

was the most intense. Some LDH-SA had also formed at 30 min (52.2 \AA). The 52.2 \AA basal reflection had a higher intensity than the 17.9 \AA (non-basal) reflection. At 60 min, however, the basal reflection reduced in intensity and interlayer distance (to 46.8 \AA), with the 17.9 \AA reflection becoming the most intense. This loss of intensity of the basal reflection may indicate that delamination and perhaps even some exfoliation took place between 30 and 60 min. We suspect that the alginate, being a poly-anionic polysaccharide [19], may have aided the exfoliation of the LDH-SA without the need for high shear mixing.

3.5. Tensile properties

The Young's modulus of the present films were an order of magnitude lower and the elongation to break an order of magnitude larger than the starch films of Wilhelm *et al.* [6] which, however, did not contain any sodium alginate. Fig. 9 shows the effect of filler composition on the Young's modulus. The highest modulus was achieved at about 60SA/40LDH. This point probably corresponded to the minimum amount of SA needed to effectively break up the sand-rose structure in order to increase the surface area and efficiency of the reinforcing interaction between the LDH and the alginate, and possibly the dextrin. After the 60SA/40LDH point the amount of LDH available became less and thus also the reinforcing capabilities. The talc and bentonite, at the same mass %, did not have the same reinforcing effect (Fig. 9). A maximum increase in Young's modulus of 213% in comparison to the blank dextrin-alginate film was attained. Wilhelm *et al.* [6] obtained only a 72% increase in modulus at 30% m/m loading of Ca^{2+} hectorite in comparison to pristine thermoplastic starch (glycerol-plasticized). De Carvalho *et al.* [5] observed a 50% increase in modulus of starch/calcined kaolin composites at 50 phr kaolin (50 parts kaolin per 100 parts thermoplastic starch) in comparison to the pristine thermoplastic starch. Hence, the reinforcing capability of the LDH can probably be attributed to the electrostatic interaction between the positively charged LDH layers and the anionic alginate chains, which is absent in the case of talc and bentonite.

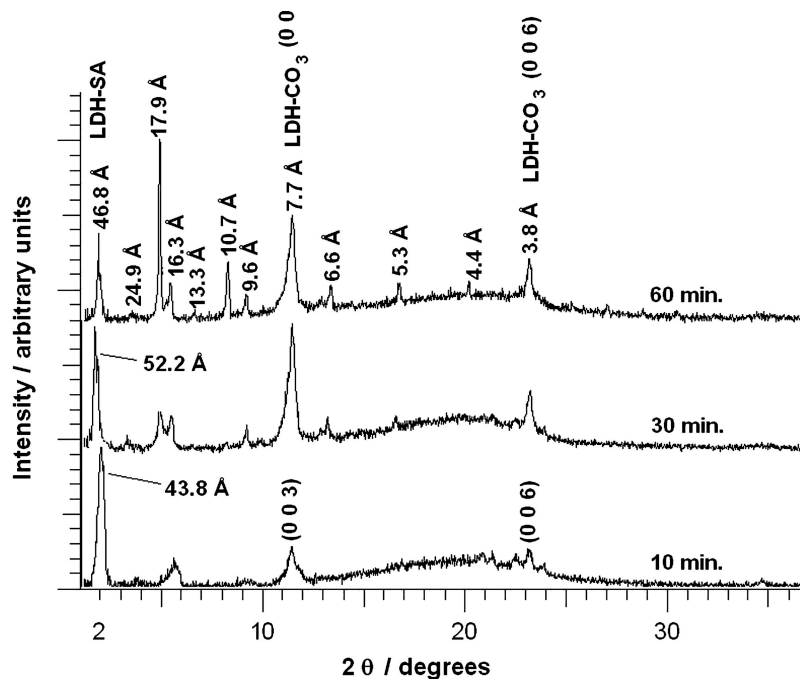


Figure 8 The crystalline phases present in the dried film 70SA/30LDH at 10, 30 and 60 min of reaction, showing the relative amounts of the LDH-CO₃ and LDH-SA phases and the lower interlayer distance LDH-SA phase remaining after exfoliation.

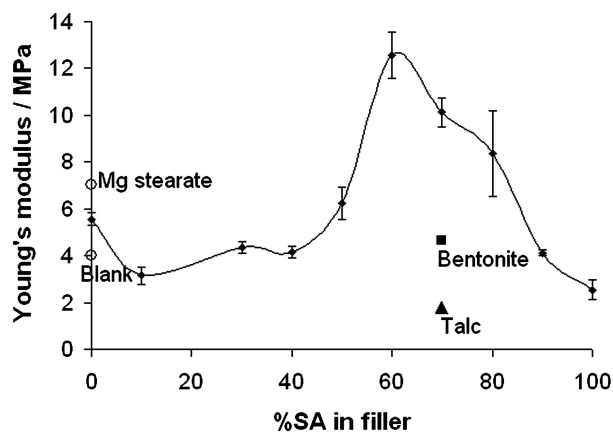


Figure 9 Young's modulus of films as function of filler composition.

4. Conclusions

The water vapour permeability (WVP) and mechanical properties of glycerol plasticized dextrin-alginate films, filled with stearate intercalated layered double hydroxides (LDH-SA), was investigated. The total filler content, comprising both the SA and the LDH, was fixed at 16.6% mass/mass of the dried films. The two filler components were allowed to react in the film casting solution for one hour. Sodium alginate acted as a dispersant and facilitated the intercalation of the stearic acid into LDH that was suspended in the water-alcohol film solution. The resultant cast film properties were not affected when either neat SA or LDH were the fillers. However, superior mechanical and barrier properties were realized at intermediate filler compositions. This coincided with the appearance

of platelet morphologies. It is concluded that the property improvements are related to the high-aspect ratio sheets of SA intercalated LDH and their interaction with the sodium alginate present in the formulation.

Acknowledgments

The financial assistance of the Department of Labour (DoL) towards this research is hereby acknowledged. Opinions expressed and conclusions arrived at, are those of the author and are not necessarily to be attributed to the DoL. The authors also wish to thank African Products (Pty) Ltd, the THRIP programme of the NRF and the Department of Trade and Industry and the University of Pretoria for financial support. The X-ray diffraction analyses done at the Council for Geoscience (South Africa) is also acknowledged.

References

1. Y. WU, C. L. WELLER, F. HAMOUZ, S. CUPPETT and M. SCHNEPF, *J. Food Sci.* **66** (2001) 486.
2. O. R. FENNEMA, S. L. KAMPER and J. J. KESTER, USP 4 915 971, Method for Making an Edible Film and for Retarding Water Transfer Among Multi-Component Food Products, 10 April 1990.
3. R. J. AVENA-BUSTILLOS and J. M. KROCHTA, *J. Food Sci.* **58** (1993) 904.
4. M. ALEXANDRE and P. DUBOIS, *Mater. Sci. Eng. R* **28** (2000) 1.
5. A. J. F. DE CARVALHO, A. A. S. CURVELO and J. A. M. AGNELLI, *Carbohydr. Polym.* **45** (2001) 189.
6. H.-M. WILHELM, M.-R. SIERAKOWSKI, G.P. SOUZA and F. WYPYCH, *ibid.* **52** (2003) 101.
7. *Idem. Polym. Int.* **52** (2003) 1035.
8. D. W. S. WONG, K. S. GREGORSKI, J. S. HUDSON and A. E. PAVLATH, *J. Food Sci.* **61** (1996) 337.
9. S. MIYATA and T. KUMURA, *Chem. Lett.* (1973) 843.

10. T. ITOH, N. OHTA, T. SHICHI, T. YUI and K. TAKAGI, *Langmuir* **19** (2003) 9120.
11. M. ADACHI-PAGANO, C. FORANO and J.-P. BESSE, *Chem. Commun.* (2000) 91.
12. A. WEXLER, in "Handbook of Physics and Chemistry," 79th ed., edited by D. R. Lide (CRC Press, Boca Raton, 1998) p. 15.
13. J. M. KROCHTA and C. DE MULDER-JOHNSTON, *Food Technol.* **51** (1997) 61.
14. M. BORJA and P. K. DUTTA, *J. Phys. Chem.* **96** (1992) 5434.
15. T. H. MCHUGH, R. AVENA-BUSTILLOS and J. M. KROCHTA, *J. Food Sci.* **58** (1993) 899.
16. T. KANO, T. SHICHI and K. TAKAGI, *Chem. Lett.* (1999) 117.
17. J. F. MEAD, R. B. ALFIN-SLATER, D. R. HOWTON and G. POPJÁK, in "Lipids: Chemistry, Biochemistry and Nutrition" (Plenum Press, New York, 1986) p. 53.
18. W. T. ASTBURY, *Nature* **155** (1945) 167.
19. R. L. WHISTLER and J. N. BEMILLER, in "Carbohydrate Chemistry for Food Scientists" (Eagan Press, St. Paul, Minnesota, 1997) p. 196.

*Received 15 April
and accepted 22 June 2005*